Silicon Nanogaps

DOI: 10.1002/ange.201102791

Synthesis of Covalently Linked Molecular Bridges between Silicon Electrodes in CMOS-Based Arrays of Vertical Si/SiO_2/Si Nanogaps**

Geoffrey J. Ashwell, Laurie J. Phillips, Benjamin J. Robinson, Susan A. Barnes, Aled T. Williams, Barbara Urasinska-Wojcik, Colin J. Lambert, Iain M. Grace, Timothy I. Cox, and Ian C. Sage*

The fabrication of nanometer-sized electrode gaps and the availability of self-assembling molecules of corresponding length[1–4] are significant challenges in the miniaturization of molecular electronic devices. To overcome the intricacy of matching these dimensions, molecular connection is facilitated by stepwise synthesis of the bridging unit within the gap itself. It affords sub-nanometer control of molecular length by self-assembly of electrode coatings that are surface reactive and next by linking smaller chemical subunits.[5–8] There are five examples of conjugated bridges formed in this way: four bridge metallic electrodes,[9–12] whereas the fifth and most recent concerns a fluorene oligomer that connects silicon electrodes.[13] In addition to bridging electrode gaps, scalability is fundamental to molecular electronic devices finding practical applications and is addressed by applying complementary metal-oxide semiconductor (CMOS) processing methods to nanogap device architectures.[13–15] Herein, we focus upon silicon electrodes; studies, albeit few to date, have resulted in contacting by C_{60} deposits within the gap[16] as well as bridging by covalently linked nanoparticles[15] and a 5.8 nm long fluorene oligomer.[13] The latter example was the first to be grafted on both sides to silicon; herein, we present the device characteristics of a second example but with a shorter 2.8 nm span. The electrode gap was bridged by grafting 4-ethynylbenzaldehyde, Si–CH=CH–C_6H_4–CHO, to activate the surfaces and, thereafter, by coupling 2,6-diaminoanthra-9,10-quinone to connect the electrode coatings on opposite sides of the gap by imine links (Figure 1). Following the initial grafting stage, the silicon nanogaps exhibit leakage currents of less than 2 pA at 1 V, but the current increases to 11–14 nA at 1 V upon molecular bridging. The process may be reversed by soaking in acidified solution, which detaches the linker unit and causes the current to diminish.

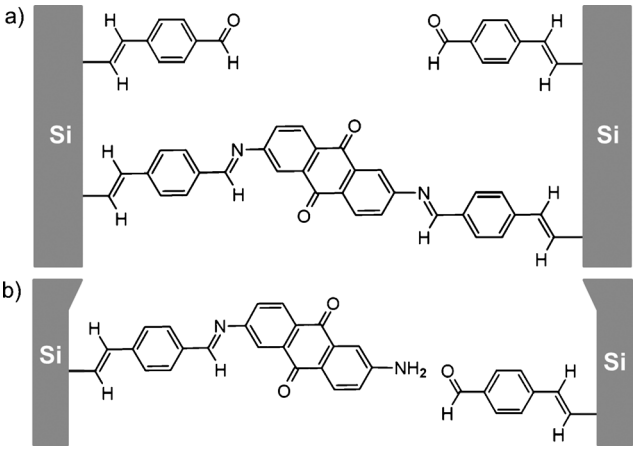

Figure 1. Reaction at the silicon surface: a) Molecular structures of the chemisorbed species and a 2.8 nm long molecular bridge formed by grafting the diethylacetal derivative of 4-ethynylbenzaldehyde and reacting the grafted molecules with 2,6-diaminoanthra-9,10-quinone at ambient temperature; b) an asymmetric nonbridging molecule coupled by an imine link to one side of the anthraquinone unit when the nanogap is too wide to accommodate the molecular bridge. The connection relies on surface roughness to match the length of the molecule to the width of the nanogap and limits the number of suitable bridging sites.

CMOS-based arrays of Si/SiO_2/Si sandwich structures with a surface density of about 700 devices cm^{-2} were fabricated as described in a previous report.[13] The electrodes are arsenic-doped Si(111) and polysilicon, and the nanosized gap, which is shown as a V-shaped opening in Figure 2, is formed by selectively etching the edge of the interfacing oxide layer. Its thickness governs the minimum width of the electrode gap, and although influenced by surface roughness, approaches 2.8 nm, which is the dimension of the bridging molecule. The length of the undercut is 10–90 μm. The undercut length was varied by altering the size and shape of the exposed region of the top silicon electrode as well as the number of undercut edges. The nanogap was created by wet etching with NH_4F solution, which hydrogenates the surface and provides electrodes that are moderately resilient to oxidation. X-ray photoelectron spectra (XPS) of samples exposed to air for 50 h exhibit Si 2p peaks at 99.0 eV (Si–Si)

[*] Prof. G. J. Ashwell, Dr. B. J. Robinson
The Nanomaterials Group, Physics Department
Lancaster University, Lancaster LA1 4YB (UK)
E-mail: g.j.ashwell@lancaster.ac.uk
Dr. L. J. Phillips, S. A. Barnes, A. T. Williams, Dr. B. Urasinska-Wojcik
Nanomaterials Group, College of Physical and Applied Sciences
Bangor University (UK)
Prof. C. J. Lambert, Dr. I. M. Grace
Condensed Matter Theory Group, Physics Department
Lancaster University (UK)
Dr. T. I. Cox, Dr. I. C. Sage
QinetiQ plc, Malvern (UK)

[**] This work was supported by the Engineering and Physical Sciences Research Council, Technology Strategy Board and EC FP7 ITN "FUNMOLS" project no. 212942. CMOS = complementary metal-oxide semiconductor.

Supporting information for this article is available on the WWW under http://dx.doi.org/10.1002/anie.201102791.

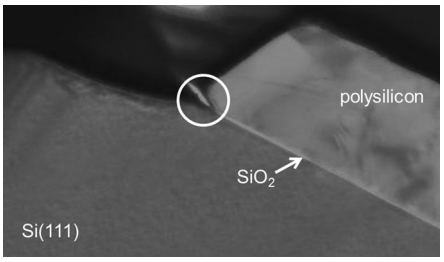

Figure 2. Scanning electron microscopy image of an $Si/SiO_2/Si$ cross-section in which the top and bottom electrodes, arsenic-doped Si(111) and polysilicon, respectively, are separated by an ultrathin SiO_2 layer. The oxide layer is etched along its outer edge to provide a nanosized electrode gap, which is illustrated within the circle by the apex of the V-shaped undercut. Although not shown by this image, the electrodes are contacted by 2 μm diameter aluminum plugs, which connect to 150 μm x 150 μm aluminum pads for contact with a probe station. For details, see the Supporting Information.

and 99.6 eV (Si–H) with only a minor peak arising from oxygen-bonded silicon. Nonetheless, the etched devices were protected immediately by chemical grafting in an inert argon atmosphere to suppress residual oxidation. The electrode surfaces were treated with the diethylacetal derivative of 4-ethynylbenzaldehyde in hexadecane (0.1 mg cm^{-1}) for 2 h at 190 °C and rinsed with copious volumes of chloroform to remove physisorbed material. Chemisorption was verified by the Si 2p core-level spectrum, which has a peak at 101.9 eV that conforms to the Si–C link, and by the Fourier-transform infrared attenuated total reflection (FTIR-ATR) spectrum which, for example, exhibits a characteristic CO stretching mode at 1703 cm^{-1} that corresponds to the aldehyde group. Analytical studies were performed on surface-treated silicon wafers, but there is no reason to assume that the etched device should not react accordingly.

Si–CH=CH–C_6H_4–CHO coatings on opposite sides of the gap permit molecular bridging of amino-terminated wires by imine links, Si–CH=CH–C_6H_4–CH=N–wire–N=CH–C_6H_4–CH=CH–Si, but the dimensions must be complementary. To achieve this, arrays of the coated devices were immersed for periods of 5 min to 2 h in THF solutions of 2,6-diaminoanthra-9,10-quinone (0.03 mg cm^{-1}) to which catalytic traces of either formic acid or acetic acid were added, then rinsed and air-dried. Direct chemical analysis of the bridged nanogap is not possible, and a proof of concept was provided instead by performing the reaction on conventional substrates, for example, large-area Si, Au, Pt, and TiO_2 surfaces as well as Au, Pt, and TiO_2 nanoparticles. Stepwise synthesis was achieved by chemisorbing molecules with surface-based aldehyde groups and next by reacting amino-terminated units and vice versa. This modular approach permits sequencing of units in a predefined manner and combines ease of synthesis with sub-nanometer control of molecular length. XPS and FTIR studies confirm that imine coupling on solid supports is independent of the underlying inorganic substrate. It is verified by a lowering of the N 1s binding energy to 398.9–399.3 eV compared with 399.9–400.3 eV for NH_2 and the loss and emergence of the CO stretching frequency of the surface aldehyde at successive reaction steps. Analytical data are included in the Supporting Information, and the binding energy shift is consistent with data reported in the National Institute of Standards and Technology XPS database.[17]

Current-voltage (*I–V*) characteristics of the molecule-inserted $Si/SiO_2/Si$ structures were obtained by using a Keithley Instruments model 6430 sub-femtoamp source meter and a Wentworth manual probe station to contact individual devices. Data were collected following the initial grafting step, and once again following attempts to bridge the silicon electrodes by coupling 2,6-diaminoanthra-9,10-quinone linker units. The former yielded leakage currents of less than 2 pA at 1 V, as expected for an open nanogap. It is independent of the size and shape of the exposed region of the silicon electrode in different devices, which is expected, as the area of overlap of the top and bottom electrodes is similar when the exposed and unexposed regions are taken into account. In this study, 98 nanogap devices were studied, of which eight shorted, and most of the remainder showed no change in their electrical behavior following immersion in solutions of the amino-terminated linker. One device exhibited a current of 0.1 nA at 1 V, which was attributed to a nonbridging arrangement, as the current is significantly lower than theoretically derived values for covalently bridged silicon devices. In contrast, reproducible *I–V* characteristics and currents of 11–14 nA at 1 V were obtained on seven occasions following immersion. These data are assigned to bridged structures, but we note that the range is narrow compared with currents of 10–10,000 nA at 1 V obtained for 5.8 nm wide molecule-inserted silicon nanogaps.[13] In both cases, we relied upon disparity between the width of the nanogap and length of the connecting molecule to minimize the number of compatible bridging sites whilst using inherent surface roughness to match the dimensions. Based on this, we suggest that the restricted current range and low yield of working devices arise from limitations imposed by this method and greater incompatibility when attempting to bridge the electrode gap with a shorter 2.8 nm long molecular wire.

We focus on a device whose *I–V* characteristics were unchanged when the immersion period in a solution of 2,6-diaminoanthra-9,10-quinone was increased from 5 min and 2 h. It exhibited a current of 12 nA at 1 V (Figure 3), showed indistinguishable behavior when studied in air and dry nitrogen, and its *I–V* characteristics were stable when cycled between ±1 V. To confirm molecular bridging, control studies were performed to decouple the unit, and thereafter, by bridging the gap to restore the current. The imine link is broken by acidified solution, as demonstrated by XPS studies, which show a 1 eV shift of the N 1s binding energy from ca. 399.0 eV (C=N) to 400.0 eV (NH_2). The anthraquinone linker in this case became detached when the silicon nanogap was soaked for 16 h in acetic acid solution (10^{-3} M). The treated device following rinsing with chloroform and drying in air exhibited a diminished current and, although not apparent from data shown in Figure 3, the horizontal line exhibits slight asymmetry with currents of 0.08 nA at −1 V and 0.03 nA at +1 V. These values are higher than the leakage current following grafting with 4-ethynylbenzaldehyde (copared with less than 2 pA at 1 V), and the slight asymmetry is assigned to

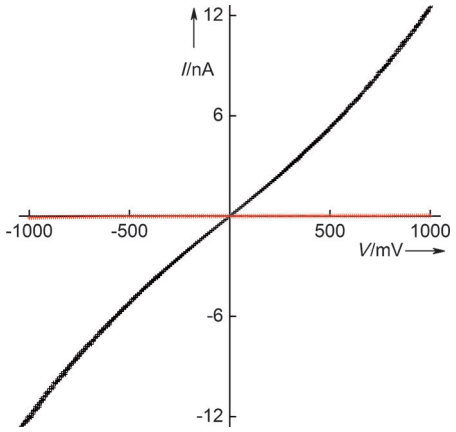

Figure 3. Symmetrical *I–V* characteristics of a bridged $Si/SiO_2/Si$ nanogap device (black) and altered behavior following immersion in an acidified solution to disconnect the anthraquinone linker unit (red). The sign is assigned to the bottom Si(111) electrode of the device and, although not discernible from the scale of the plot, the currents at 1 V differ by a factor of 150 in the negative quadrant and a factor of 400 in the positive quadrant (see the Supporting Information).

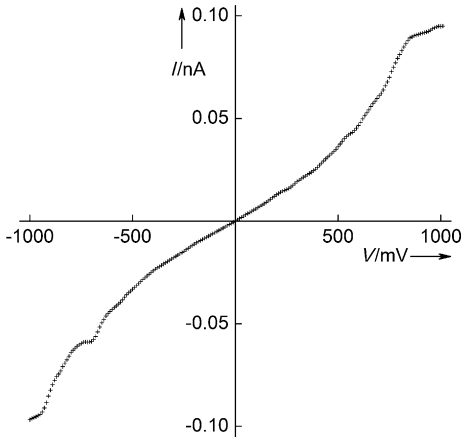

Figure 4. *I–V* curve of an $Si/SiO_2/Si$ nanogap device, the current of which is at the lower limit of those observed when the 4-ethynylbenzaldehyde grafted electrodes are treated with 2,6-diaminoanthra-9,10-quinone. Anomalous distortions in the electrical characteristics are attributed to a nonbridging arrangement, with altered contacting distances induced by rotation about the exocyclic single bonds of the molecule as the voltage is swept.

incomplete exclusion of the electron-accepting linker. The current is higher when the bottom Si(111) electrode is negatively charged (cathode), and based on the behavior of molecular diodes[18] and organic rectifying junctions,[19] it may be assumed that an electron-accepting anthraquinone moiety is located on this side of the device (as shown for example in Figure 1 b). However, regardless of explanation, the control study shows profound changes in electrical behavior for conditions that reverse the bridging process. It supports our premise that the current of 12 nA at 1 V is not an experimental artifact but inherent to the bridged Si-molecule-Si nanogap (Figure 1 a). Besides, we reject the prospect of the behavior arising from trapped molecular deposits because rinsing repeatedly with copious volumes of solvent has no effect on the magnitude of the current or *I–V* characteristics.

We now turn to a molecule-inserted nanogap whose current is at the lower limit of those measured. The current of 0.1 nA at 1 V is seven times smaller than the theoretically derived value for a single molecular bridge, and unlike the smooth curve shown in Figure 3, the *I–V* characteristics exhibit deformations as the voltage is swept between ± 1 V (Figure 4). The magnitude makes it necessary to consider a nonbridging structure with either an interdigitating arrangement of molecules or a suitably narrow gap between the electrode coatings. The anomalous behavior probably results from single points of attachment. If the molecules anchor at one end, irregularities in the *I–V* profile may be explained by rotation of the subunits about their exocyclic single bonds and subtle changes in intermolecular contacting distances across the nanogap. Bridging is reliant on an exact match between the width of the gap and length of the stepwise-formed molecular bridge. Therefore, attempts were made to connect the electrodes of this device by longer molecules, for example, by coupling amino-terminated units, $H_2N{-}wire{-}NH_2$, followed by terephthalaldehyde, $OHC{-}C_6H_4{-}CHO$, and thereafter by repeating these steps. However, the process had no discernable effect on the current or shape of the *I–V* curves of both the bridged (Figure 3) and unbridged devices (Figure 4). It may be assumed that the width of the electrode gap, which is dependent upon the thickness of the preformed oxide spacer layer, is reasonably similar throughout the array of silicon nanogaps, and serendipity plays a role in matching its dimensions to those of the molecule.

Ab initio transport code SMEAGOL[20] and density functional (DFT) code SIESTA[21] were used to predict the electrical transport properties of the silicon-contacted molecule. The relaxed geometry of the isolated molecule and optimum binding geometry to the silicon surface were calculated using DFT. It was extended to include 6 layers of Si(111), each containing 25 atoms, which were attached to infinite periodic leads. Periodic boundary conditions were imposed in the x and y directions (the transport axis is along z), and a silicon lead structure was chosen to mimic the doped behavior, that is, with a finite density of states at the Fermi energy. The zero bias electron transmission coefficient, $T(E)$, was calculated using SMEAGOL (Figure 5), and the *I–V* relation (Figure 6) was obtained from $T(E)$ using Equation (1):

$$I = \frac{2e}{h} \int_{eV}^{eV/2} T(E)\mathrm{d}E \qquad (1)$$

Profiles of the *I–V* curves from theory and experiment are alike, but their currents, 0.7 nA at 1 V (Figure 6) and 12 nA at 1 V (Figure 3), differ by a factor of seventeen. This may be explained in part by a few molecular bridges rather than a single molecule bridging the gap. For so few molecules, as indicated by the modest difference, the likelihood of clustering is remote when these silicon nanogaps may be bridged along 10–90 μm lengths. We also note that discrepancies probably arise from problems associated with the use of DFT

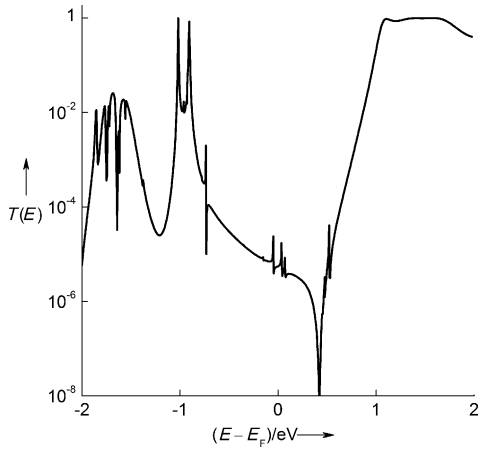

Figure 5. Theoretical transport properties: zero bias transmission coefficient of the 2.8 nm long molecular wire contacted by silicon leads as a function of $E-E_F$, where E_F is the Fermi energy and E is the energy of the transmitted electrons.

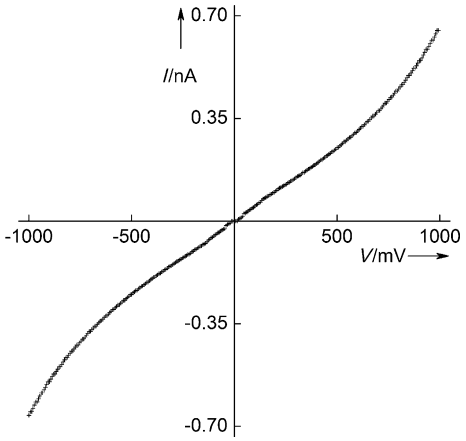

Figure 6. Theoretical *I–V* characteristics: the gentle reverse-S profile of the *I–V* curve of the silicon-contacted 2.8 nm long molecular wire mimics the experimental curve shown in Figure 3.

to estimate the HOMO–LUMO gap and the position of the Fermi energy as well as to difficulties in simulating the Si-molecule-Si device characteristics when the electrodes are highly doped and asymmetric in their morphology. The top and bottom electrodes are arsenic-doped polycrystalline silicon and Si(111), respectively. Difficulties arise from a theoretical viewpoint as there are unknown parameters at an atomic scale that probably contribute to the discrepancy between the estimated and experimentally determined currents. Details of the theoretical method is included in the Supporting Information.

In summary, there is one previous report of the electrical characterization of a molecule grafted at each end to silicon electrodes.[13] In this work, we describe a second, albeit much shorter example, in which the bridging of silicon nanogaps is achieved by a 2.8 nm-long molecular wire. Reproducible currents and *I–V* characteristics following multiple rinsing cycles in chloroform confirms that the behavior does not arise from molecular deposits. In the same way, suppression of the current following immersion in acidified solution is symptomatic of the molecular bridging unit becoming detached as imine links break under these conditions. It suggests that the current of about 12 nA at 1 V (compared with less than 2 pA at 1 V following the initial grafting step) is inherent to the Si-molecule-Si bridge. In this case, the stepwise synthesis of molecular wires within the silicon nanogap itself with covalent bonding to the electrodes on opposite sides is fundamental to matching the respective dimensions. The process has been applied herein to CMOS-based arrays, and the scalability of the technique, that is, the mass production of silicon nanogaps combined with an in situ modular approach for bridging the electrodes, points the way to molecule-inserted test-bed structures for silicon-based electronics. There is reasonable agreement between the experimental and theoretical *I–V* characteristics for the bridged device, and our studies have shown it to be robust when cycled between ± 1 V.

Received: April 21, 2011
Revised: May 24, 2011
Published online: July 26, 2011

Keywords: molecular electronics · nanogaps · nanotechnology · self-assembly · semiconductors

[1] X. Chen, Z. Guo, G.-M. Yang, J. Li, M.-Q. Li, J.-H. Liu, X.-J. Huang, *Materials Today* **2010**, *13*, 28 – 41.
[2] T. Li, W. Hu, D. Zhu, *Adv. Mater.* **2010**, *22*, 286 – 300.
[3] A. K. Feldman, M. L. Steigerwald, X. Guo, C. Nuckolls, *Acc. Chem. Res.* **2008**, *41*, 1731 – 1741.
[4] a) S. Strobel, R. M. Hernández, A. G. Hansen, M. Tornow, *J. Phys.: Condens. Matter.* **2008**, *20*, 374126; b) R. Søndergaard, S. Strobel, E. Bondgaard, K. Norman, A. G. Hansen, E. Albert, G. Csaba, P. Lugli, M. Tornow, F. C. Krebs, *J. Mater. Chem.* **2009**, *19*, 3899 – 3908.
[5] T. P. Sullivan, W. T. S. Huck, *Eur. J. Org. Chem.* **2003**, 17 – 29.
[6] N. Tuccitto, V. Ferri, M. Cavazzini, S. Quici, G. Zhavnerko, A. Licciardello, M. A. Rampi, *Nat. Mater.* **2009**, *8*, 41 – 46.
[7] a) S. H. Choi, C. Risko, M. C. Ruiz Delgado, B. Kim, J.-L. Bredas, C. D. Frisbie, *J. Am. Chem. Soc.* **2010**, *132*, 4358 – 4368; b) L. Luo, C. D. Frisbie, *J. Am. Chem. Soc.* **2010**, *132*, 8854 – 8855.
[8] a) G. J. Ashwell, B. Urasinska-Wojcik, L. J. Phillips, *Angew. Chem.* **2010**, *122*, 3586 – 3590; *Angew. Chem. Int. Ed.* **2010**, *49*, 3508 – 3512; b) G. J. Ashwell, A. T. Williams, S. A. Barnes, S. L. Chappell, L. J. Phillips, B. J. Robinson, B. Urasinska-Wojcik, P. Wierzchowiec, I. R. Gentle, B. J. Wood, *J. Phys. Chem.* C **2011**, *115*, 4200 – 4208.
[9] M. Taniguchi, Y. Nojima, K. Yokota, J. Terao, K. Sato, N. Kambe, T. Kawai, *J. Am. Chem. Soc.* **2006**, *128*, 15062 – 15063.
[10] a) G. J. Ashwell, P. Wierzchowiec, C. J. Bartlett, P. D. Buckle, *Chem. Commun.* **2007**, 1254 – 1256; b) G. J. Ashwell, P. Wierzchowiec, L. J. Phillips, C. Collins, J. Gigon, B. J. Robinson, C. M. Finch, I. R. Grace, C. J. Lambert, P. D. Buckle, K. Ford, B. J. Wood, I. R. Gentle , *Phys. Chem. Chem. Phys.* **2008**, *10*, 1859 – 1866.
[11] J. Tang, Y. Wang, J. E. Klare, G. S. Tulevski, S. J. Wind, C. Nuckolls, *Angew. Chem.* **2007**, *119*, 3966 – 3969; *Angew. Chem. Int. Ed.* **2007**, *46*, 3892 – 3895.
[12] X. Chen, A. B. Braunschweig, M. J. Wiester, S. Yeganeh, M. A. Ratner, C. A. Mirkin, *Angew. Chem.* **2009**, *121*, 5280 – 5283; *Angew. Chem. Int. Ed.* **2009**, *48*, 5178 – 5181.
[13] G. J. Ashwell, L. J. Phillips, B. J. Robinson, B. Urasinska-Wojcik, C. J. Lambert, I. M. Grace, M. R. Bryce, R. Jitchati, M. Tavasli,

T. I. Cox, I. C. Sage, R. P. Tuffin, S. Ray, *ACS Nano* **2010**, *4*, 7401 – 7406.
[14] S. M. Dirk, S. W. Howell, S. Zmuda, K. Childs, M. Blain, R. J. Simonson, D. R. Wheeler, *Nanotechnology* **2005**, *16*, 1983 – 1985.
[15] S. W. Howell, S. M. Dirk, K. Childs, H. Pang, M. Blain, R. J. Simonson, J. M. Tour, D. R. Wheeler, *Nanotechnology*, **2005**, *16*, 754 – 758.
[16] D. A. Corley, T. He, J. M. Tour, *ACS Nano* **2010**, *4*, 1879 – 1888.
[17] National Institute of Standards and Technology X-ray photoelectron spectroscopy database (http://srdata.nist.gov/xps/default.aspx).
[18] G. J. Ashwell, A. Mohib, *J. Am. Chem. Soc.* **2005**, *127*, 16238 – 16244.
[19] G. J. Ashwell, B. Urasinska, W. D. Tyrrell, *Phys. Chem. Chem. Phys.* **2006**, *8*, 3314 – 3319.
[20] A. R. Rocha, V. M. Garcia-Suarez, S. Bailey, C. Lambert, S. Sanvito, J. Ferrer, *Phys. Rev. B* **2006**, *73*, 085414.
[21] J. M. Soler, E. Artacho, J. D. Gale, A. Garcia, I. Junquera, P. Ordejon, D. Sanchez-Portal, *J. Phys.: Condens. Matter* **2002**, *14*, 2745 – 2779.

